Construction and Building Materials 407 (2023) 133473

Contents lists available at ScienceDirect

Construction and Building Materials

journal homepage: www.elsevier.com/locate/conbuildmat

A study on permanent deformation and fatigue damage interaction in asphalt concrete

Mequanent Mulugeta Alamnie [a,*], Ephrem Taddesse [a], Inge Hoff [b]

[a] Department of Engineering Sciences, University of Agder, Grimstad 4879, Norway
[b] Department of Civil and Environmental Engineering, Norwegian University of Science and Technology, Trondheim 7491, Norway

ARTICLE INFO

Keywords:
Permanent Deformation
Fatigue
Sequential Test
Dissipated Energy
Continuum damage
Flow Number

ABSTRACT

The dominant load-induced damages, permanent deformation (PD) and fatigue cracking (F), are traditionally predicted separately by taking temperature as a variable of departure. This paper presents an experimental study of the two damages and interaction using sequential test procedure (STP) based on 'sequential damage'. The STP is conducted in PD-F and F-PD sequences on each specimen using a creep-recovery and cyclic fatigue tests. The effect of strain hardening on fatigue cracking is studied in the PD-F sequence, and the impact of fatigue cracking on permanent deformation is explored using the F-PD sequence. First, the shear deformation in tertiary stage of creep recovery is investigated using the dissipated energy ratio criterion and a new fourth creep phase is obtained. Following the PD-F sequence, strain-hardening is found a significant accelerator of fatigue damage rate, particularly on aged and laboratory produced mixes. The fatigue tests without considering the strain-hardening effect underestimate fatigue damage rate. In the F-PD sequence, the effect of pre-existing crack (up to 40% modulus reduction) on permanent deformation is found marginal. The sequential test and damage approach is an effective way to analyze interaction between damage modes and evaluate asphalt mixtures.

1. Introduction

Asphaltic concrete is a crucial pavement material with a viscoelastic and viscoplastic behavior under different strain levels and temperature conditions. Pavement structures are typically exposed to high magnitude, complex mechanical, and environmental loads. The complex tire-pavement interface stress and environmental factors caused different modes of damage in asphalt pavements. The damage on the pavement is manifested in the form of energy dissipation, material ductility exhaustion, cracking, hardening, and viscoplastic flow. Among the different damage modes, permanent deformation and fatigue cracking are the two dominant damage mechanisms. At the material level, the constituents of asphalt mixture (aggregates, binder, and air voids) and confinement have significant effect on the respective damage mechanisms [1,2].

Permanent deformation (or rutting) in asphalt layer is caused by the accumulation of non-recoverable (viscoplastic) strain under repeated traffic loading, mainly at elevated temperatures. At structural level, permanent deformation is related to three mechanisms: (1) viscoplastic deformation in the asphalt layer (densification and shear flow), (2) the sub-structural (subbase and subgrade) settlement, and (3) studded tire abrasion in the wheel path [3–5]. At the mixture level, the permanent strain is accumulated because of microstructure changes in the asphalt mixture matrix under a creep-recovery cycle. A strain hardening-relaxation phenomenon is one of the behaviors of asphalt concrete. The merits of considering the hardening-relaxation behavior is to consider the load history effect in the model and to capture a variable hardening rate at each loading cycle [6–8]. However, the permanent deformation modeling is heavily relayed on the data from a standard repeated creep-recovery test. The accumulated permanent strain at the end of each creep-recovery cycle is described in three distinct stages: *primary, secondary and tertiary* [9,10]. The primary creep stage is characterized by a rapid deformation at a decreasing rate (volumetric densification), and the secondary stage (steady state) has a constant viscoplastic strain rate. The viscoplastic strain hardening reaches saturation at the flow number and the tertiary creep commences with a rapid shear deformation [11]. At the maximum strain hardening saturation, the extra energy is consumed to initiate microcracks (viscodamage) and an increase in phase angle [12].

Fatigue damage, on the other hand, is a stiffness deterioration mechanism due to the formation and propagation of cracks under cyclic stress- or strain-control load. Several fatigue test protocols were

* Corresponding author.
E-mail address: mequanent.m.alamnie@uia.no (M.M. Alamnie).

https://doi.org/10.1016/j.conbuildmat.2023.133473
Received 16 March 2023; Received in revised form 6 September 2023; Accepted 19 September 2023
Available online 27 September 2023

attempted such as the indirect tensile, beam bending, and axial loading scenarios [13,14]. The traditional fatigue design criterion was based on the critical tensile strain at the bottom of the asphalt layer and the crack propagates bottom-up (BUC). The BUC is mainly due to structural problems not load-related. Studies showed that load related fatigue cracks started at or near the pavement surface and propagated downwards, that is, top-down cracking (TDC). Although researchers have reached different conclusions regarding the causes and locations of TDC, it is believed that TDC is caused by high radial tensile stress at the surface and longitudinal cracks in wheel paths [15–18]. Furthermore, experimental and field observations showed that TDC is critical in medium and thick asphalt layers, and BUC is dominant in thin pavements. It is also argued that the BUC appears as disintegrated zones (cannot reach the surface), and can conjoined and coalesce with TDC [19]. Furthermore, differential stiffness in the surface and base layers of asphalt pavement, and rutting of substructure layers can cause significant tensile stresses at the surface and bottom of asphalt pavement layer that leads to both TDC and BUC. This means design based on tensile strain at the bottom of asphalt layer overestimates fatigue life.

Nevertheless, an interaction of permanent deformation and fatigue cracking (TDC or BUC) in asphalt concrete has never been studied in detail and little is known about the simultaneous damage evolution. Current fatigue and permanent deformation models (both energy- or continuum- based) are based the assumption of mutually independent (non-associated) damage evolution. Temperature is often taken as a boundary thermodynamic variable between fatigue and permanent deformation. This is because asphalt relaxes faster at high temperature and become fatigue cracking resistant, and the stiffness (elasticity) increase at low temperature where permanent deformation is insignificant [20]. This distinction can be accurate in a controlled test at fixed temperature. However, the interaction between the two main damages is inevitable in actual pavement due to the reasons: (1) pavement temperature varies significantly in a day let alone over seasons, (2) the same load causes both damages, (3) as a viscoelastic-viscoplastic material, pure cracking never happen and plastic deformation around localized regions of cracks also evolves simultaneously, regardless of the temperature [21]. Hence, pure cracking and pure permanent deformation is unlikely by varying the temperature or loading level. Based on field observations, surface deformation along the wheel path causes longitudinal surface cracking inside or just outside of wheel-path [16,17,22]. Furthermore, as a three-phase material, the air voids are the most important components of asphalt mixture morphology, and about 4% void content is generally provided to prevent early rutting failure. The air voids can be considered as multitude of distributed pre-existing cracks [23]. For example, air void contents of 4% and 7% corresponds to pre-existing crack size of 0.65 mm and 0.79 mm, respectively [24]. When external load is applied, stress concentrates around the pre-existing flaws (air voids), and wing cracks initiate and propagate parallel to the load direction. Thus, the air voids can act as point of crack initiation due to tension–tension or tension–compression load and viscodamage cracking due to compression [25]. These observations are testimonial for the association of fatigue cracking and the accompanying permanent deformation.

This paper is focused on the experimental study of permanent deformation and fatigue damage, and the effect of one damage evolution on another. The interaction between the two damage modes is analyzed by following a sequential test procedure in two orders [26]: (1) the permanent deformation – fatigue (PD-F) damage sequence, (2) the fatigue – permanent deformation (F-PD) sequence. The PD-F sequence is to incorporate pre-deformation or strain hardening on fatigue response and the F-PD sequence is to simulate the fatigue damage development prior to permanent deformation in certain cases. In cold climate regions (seasons) and thick pavements, fatigue can develop without or prior to viscoplastic deformation. Then, fatigue cracked pavements can then undergo permanent deformation due to phase angle increment. Seven asphalt concrete mixtures were tested and analyzed in this study and the viscoelastic, viscoplastic and damage responses were studied using uniaxial dynamic modulus, repeated creep-recovery, and uniaxial fatigue tests.

2. Viscoelastic, viscoplastic and damage modeling

2.1. Viscoelastic model

Asphalt concrete behaves in linear viscoelastic manner at specific strain levels [27,28]. The strain limits for linear viscoelastic response limit was assumed different values in the ranges between 50 to 150 micro-strains. The dynamic (complex) modulus $|E^*|$ is a fundamental material property using to analyze the viscoelastic response of asphalt concrete. It is expressed in a complex number form that represents the viscous and elastic components of modulus. The frequency-, stress- and temperature-dependent properties of asphalt concrete can be characterized by constructing a dynamic modulus master curve [29]. The true stress–strain constitutive equation cannot be expressed using the dynamic modulus, which contains an imaginary component. The relaxation function E(t) is used to define the fundamental stress–strain constitutive relationship using true viscoelastic strain ε^{ve} or pseudo strain ε_i^R and pseudo stiffness (C).

$$\sigma^{ve} = \int_0^t E(t-\tau)\frac{\partial \varepsilon^{ve}}{\partial \tau}d\tau \tag{1}$$

$$\sigma = C\varepsilon_i^R = C\left(\frac{1}{E_R}\int_0^t E(t-\tau)\frac{\partial \varepsilon^{ve}}{\partial \tau}d\tau\right) \tag{2}$$

where E_R is reference modulus (in unit modulus).

Asphalt concrete is a rate dependent material, and the viscoelastic properties are not adequate to fully characterize its responses beyond the viscoelastic stress limit (σ^{ve}) under different modes of loading.

2.2. Viscoplastic model

Viscoplasticity is the response beyond linearity limit where a rate-dependent viscoplastic strain is accumulated under repetitive loadings. In a creep-recovery test with rest period, the viscoplastic strain is conventionally determined by the additive decomposition of total strain or from experiment measurement of the nonrecoverable strain. Luo et al. [30] applied the decomposition technique for direction tension mode in a pseudo strain space. As a viscoelastic-viscoplastic material, a true separation between the viscoelastic (ε^{ve}) and viscoplastic (ε^{vp}) strain is difficult with short rest period using a haversine loading pulse [31]. A coupled viscoelastic-viscoplastic analysis is the accurate way to model permanent deformation. Several research have been conducted on the viscoplastic evolution inspired by the phenomenological, microscopic or macroscopic responses of viscoplastic strain due to external loads [32]. However, most of the existing modeling approaches are focused on prediction of permanent strain data from the creep-recovery test using empirical and mechanistic-empirical equations [33]. The classic uniaxial viscoplastic flow rate (strain-hardening) model assumes a power law in viscoplasticity [34,35].

$$\dot{\varepsilon}_{vp} = \frac{g(\sigma)}{\lambda} \tag{3}$$

where $g(\sigma)$ is stress function, $\lambda = G\varepsilon_{vp}^{p}$ is viscosity parameter approximated by a power form, G and p are model coefficients. Power-based models can approximate the secondary or steady-state creep strain with good accuracy. However, power function has inherent limitation to fit viscoplastic strain in the tertiary stage (viscodamage phase). Several other empirical and mechanistic-empirical models were proposed for all creep phases [10,11]. The Francken model is the most widely applied

three-stage model, such as in AASHTO standard. The model takes the following form.

$$\varepsilon_{vp} = AN^B + C\left(e^{DN} - 1\right) \tag{4}$$

where *A, B, C and D* are coefficients and N is the number cycles. In the model, parameter *'B'* is the rate of strain hardening in the secondary stage and C indicates the start of tertiary stage (or flow number). Such type of models overrides the mechanistic and microscopic aspects of viscoplasticity and relied on the quality of creep-recovery test data, rest period between creep cycles and other control variables like temperature, confinement, axial stress magnitude, and mixture properties.

2.3. The continuum damage model

Viscoelastic continuum damage (VECD) theory is widely applied for asphalt concrete, which is derived based on Schapery's elastic–viscoelastic correspondence principle and work potential theory [36,37]. The theory utilizes internal state variable (S) to model damage. The damage variable (S) represents microstructural changes that leads to a reduction in effective stiffness due to cracking. The damage rate is defined using the maximum pseudo strain energy (W^R) and damage coefficient α as follows.

$$\frac{dS}{dt} = \left(-\frac{\partial W^R}{\partial S}\right)^{\alpha} \tag{5}$$

$$W^R = \frac{1}{2}\sigma\varepsilon_i^R = \frac{1}{2}C(S)\left(\varepsilon_i^R\right)^2 \tag{6}$$

$$C(S) = \frac{\sigma}{\varepsilon_i^R} \tag{7}$$

The parameter α is a unique material property related to viscoelastic damage evolution [38], which is dependent on the maximum slope (m_o) of relaxation modulus curve ($\alpha = \frac{1}{m_o} + 1$ for controlled-strain fatigue test). The detail formulation of simplified VECD (S-VECD) model is presented in previous studies [39–42]. The accumulated damage after one load cycle (ΔS) takes the following form.

$$\Delta S = \left[-\frac{DMR}{2}\left(\varepsilon_{a,i}^R\right)^2\left(C_i^* - C_{i+1}^*\right)\right]^{\frac{\alpha}{1+\alpha}}\left(\Delta t_R\right)^{\frac{1}{1+\alpha}} \tag{8}$$

$$\varepsilon_{a,i}^R = \frac{(\beta+1)}{2}\varepsilon_{pp} \tag{9}$$

$$DMR = \frac{|E^*|_{fingerprint}}{|E^*|_{LVE}} \tag{10}$$

$$\Delta t_R = \frac{1}{a_T}\left[\frac{\Delta N}{10}\right] \tag{11}$$

The C - S relationship (Eqn (8)) combines the effects of strain level, temperature, sample variability, and frequency.

where, *DMR* is the dynamic modulus ratio used to normalize specimen-to-specimen variation,

E^*_{LVE} is dynamic modulus from linear viscoelastic test,

$|E^*|_{fingerprint}$ is fingerprint dynamic modulus),

$\varepsilon^R_{a,i}$ is the pseudo strain amplitude,

$\beta = \frac{\sigma_{mean}}{\sigma_{pp}}$ is a load form factor,

ε_{pp} and σ_{pp} are peak-to-peak strain stress amplitudes (respectively),

σ_{mean} mean stress,

Δt_R is a reduced time of a cycle,

ΔN is the number of load cycles between two successive strain amplitudes.

2.4. Energy approach

Dissipated energy (DE) in a cyclic load is the area under the stress–strain hysteresis loop (or the work done per cycle), which is expressed by the following integral.

$$DE = \int_0^{\tau}\sigma(t)\frac{\partial\varepsilon(\tau)}{\partial\tau}d\tau \tag{12}$$

The energy expended due to applied sinusoidal, creep or creep-recovery type of loadings can be formulated by substituting the appropriate strain rate and stress functions in Eqn (12). For a controlled-strain cyclic fatigue test with a sinusoidal stress $\sigma(t) = \sigma_o sin(\omega t + \varphi_i)$ and strain $\varepsilon(t) = \varepsilon_o sin(\omega t)$ functions, the dissipated energy takes the following form.

$$DE_F = \pi E_i^* \varepsilon_i^2 sin(\varphi_i) \tag{13}$$

E_i^* is the apparent dynamic modulus at i^{th} cycle, φ_i is the phase angle, ε_o is target strain amplitude. The dissipated energy was computed by decomposing into elastic, viscous and viscoplastic (if any) stress–strain components [21,43]. Masad et al. [43] have identified three dissipated pseudo strain energy (DPSE) components: (1) energy dissipated due to increase in the apparent phase angle and the hysteresis loop, (2) dissipated energy related to permanent deformation (viscoplastic strain) and (3) change in pseudo stiffness due to damage. They also concluded that the second component of dissipated energy is less than 5 % of the change of dissipated energy between an idealized hysteresis loop and a hysteresis area with some creep-recovery strain. On the other hand, the dissipated energy due to creep (i.e., constant strain rate) is $DE_{Creep} = \sigma_o{}^*\varepsilon_{cr}$. For creep-recovery permanent deformation (DE_{PD}), creep damage accumulates only during the creep phase of a creep-recovery cycle. Thus DE_{PD} is expressed using the Francken model as follows.

$$DE_{\mathrm{PD}} \cong \sigma_{\mathrm{o}}\left(AN^{\mathrm{B}} + \mathrm{CD}\left(\mathrm{e}^{\mathrm{DN}} - 1\right)\right) = \sigma_{\mathrm{o}}{}^*\varepsilon_{vp} \tag{14}$$

The dissipated energy ratio (DER) criteria were proposed as failure indicator for asphalt concrete [44–46]. The common one is expressed as follows.

$$DER = n\left(\frac{DE_1}{DE_n}\right) \tag{15}$$

where DE_1 and DE_n are the dissipated energies at the first and the n^{th} load cycle. The DER for a controlled-strain (ε_o) cyclic fatigue (DER_F) and for creep-recovery permanent deformation (DER_{PD}) can be expressed as follows.

$$DER_F = n \times \frac{\pi E^*{}_1 \varepsilon_1^2 \sin\varphi_1}{\pi E^*{}_i \varepsilon_i^2 \sin\varphi_i} \approx n\left(\frac{E_1}{E_i}\right)\left(\frac{\varphi_1}{\varphi_i}\right) \tag{16}$$

$$DER_{PD} = N\left(\frac{\mathrm{A} + \mathrm{C}(\mathrm{e}^{\mathrm{D}} - 1)}{AN^{\mathrm{B}} + \mathrm{CD}(\mathrm{e}^{\mathrm{DN}} - 1)}\right) = N\left(\frac{K}{\varepsilon_{vp}}\right) \tag{17}$$

where $\mathrm{K} = \mathrm{A} + \mathrm{C}\left(\mathrm{e}^{\mathrm{D}} - 1\right)$ is constant, which is dependent on stress level, initial deformation, and tertiary stage shear failure rate (C and D).

3. Test Methods, and material

3.1. Materials

In this study, seven asphalt concrete mixtures were evaluated for testing. Four of the mixtures were collected from two asphalt mix production plants in Norway (denoted as P1 and P2). The mixtures are asphalt concrete (AC) and stone mastic asphalt (SMA) mixtures, as shown in Table 1. Moreover, two mixes were produced in the laboratory (designated as AC-L and SMA-L). The AC-P1 mixture is pure binder and the AC-P1-X is a polymer modified mixture. Similarly, the SMA-P2

Table 1
Tested asphalt mixtures compositions (aggregate gradation and binder properties).

Mix Type	Sieve size (mm)							Binder Content (%)	Binder Grade (at 25 °C)
	16	11.2	8	4	2	0.25	0.063		
Percent passing (%)									
Plant-Produced mixtures (P1 and P2)									
AC-P1	100	95	75	47.5	33.5	11.5	8	5.6	70/100
AC-P1-X	100	95	70	48	36	15.5	7	5.8	PMB 65/105–60
SMA-P1	100	94	56	36	27	16	10.5	5.83	70/100
SMA-P2	100	92	58	37	23	13	9	5.95	"
SMA-P2-X	100	91.2	53.6	35.7	21.7	12.8	8.4	5.83	"
Laboratory-Produced mixtures (L)									
AC-L	100	95	70	47.5	33.5	12.5	7.5	5.1	70/100
SMA-L	100	95	55.5	37.5	26	16	11	5.3	"

mixtures were sampled at different times from mixing plant 2, denoted as SMA-P2 and SMA-P2-X. Two of the mixtures, AC-P1-X and SMA-P2-X are one year older (aged) than the other mixtures. The samples were stored up to one year at room temperature. All mixtures have a nominal maximum aggregate size (NMAS) of 11 mm with pure binder except a polymer modified (PMB) for AC-P1-X.

3.2. Test methods

Cylindrical test specimens of size about 180 mm height and 150 mm diameter were produced using a gyratory compactor according to Superpave gyratory compaction procedure. The final test specimens were fabricated by coring and cutting to 150 mm height and 100 mm diameter. The IPC global universal testing machine (UTM-130) was used for testing according to the test parameters given in Table 2.

Three main types of tests were conducted to characterize asphalt mixture's viscoelastic, viscoplastic and fatigue responses. The tests are: (1) the dynamic modulus test to determine linear viscoelastic characteristics (AASHTO T378 2017), (2) a controlled-strain uniaxial fatigue test (AASHTO TP-107 2017) in both tension–tension and tension–compression modes, and (3) cyclic creep-recovery tests (EN 12697–25 2016 and AASHTO T378 2017).

3.2.1. Sequential test approach

Inspired by the sequential creep and fatigue damage evolution in researches by [47,48], the sequential test was proposed in this study to investigate the effects of permanent deformation on fatigue damage evolution and vice versa [26]. To simulate the effect of one damage mode on the other, the test campaign is performed in two sequences on each test specimen – *the PD-F* and *F-PD sequences*. The permanent deformation – fatigue (PD-F) is intended to capture the early life permanent deformation (hardening) before fatigue started. In other words, permanent deformation is a short- and fatigue is a long- term (in ranges of 10^6 cycles) damage after aging. In most cases, except thermal cracking, viscoplastic strain accumulates before fatigue cracking initiates, and permanent deformation is believed to be the cause of surface cracking in pavement [16]. In the PD-F sequence, virgin specimens are tested in a creep-recovery test within the steady-state stage well before flow number (FN) commences i.e., N < FN. Then, the pre-deformed (strain-hardened) specimens are tested in uniaxial fatigue at low temperatures until failure.

Table 2
Summary of test parameters, controls, and variables.

	Test Types		
	Dynamic modulus	**Creep-recovery**	**Uniaxial Fatigue**
Test Standard	AASHTO T378	EN 12697–25	AASHTO TP107
Specimen size (height to diameter ratio)	1.5	1.5	1.5
Number of duplicates	4	3	2
Temperature, °C	−10, 5, 10, 21, 40	30, 40, 50	10, 15, 21, 30
Frequency, Hz	20, 10, 5, 2, 1, 0.5, 0.2, 0.1	–	10
Control mode	Control strain (με): 50	Control stress (MPa): 0.5 to 2	Target strain (με): 100, 150, 200, 300, 400
Loading (rest) time, s	–	0.1 (0.9)	–
Pulse (Confinement)	Sinusoidal (*Uniaxial*)	Haversine (*Uniaxial and triaxial*)	Sinusoidal (*Uniaxial*)

The fatigue – permanent deformation (F-PD) sequences is proposed to simulate the effect of preexisting fatigue cracking on permanent deformation mechanism of asphalt concrete. In this sequence, new specimens are first tested in the uniaxial fatigue test (in tension–compression T-C or tension–tension T-T modes) in controlled-strain modes at low and intermediate temperatures (not more than 40 % of initial stiffness reduction). A 50 % initial modulus reduction due to fatigue cracking has been considered as failure indicator in asphalt concrete [13,49]. Then, the pre-fatigued specimens are tested in creep-recovery tests at elevated temperatures.

The nondestructive fingerprint dynamic modulus test was performed before the fatigue damage tests. The overall testing process is illustrated in Fig. 1, and the ball and socket joint system for uniaxial cyclic fatigue test scheme is shown in Fig. 2. A plastic steel putty epoxy was used to glue the top and bottom tension platens.

4. Results and discussions

4.1. Dynamic modulus test

The dynamic modulus maser curve is fitted using a sigmoid function and the WLF [50] time–temperature shift factor α_T through the least square optimization technique.

$$log|E^*| = \delta + \frac{(\alpha - \delta)}{1 + exp(\eta - \gamma log f_R)} \tag{18}$$

$$\log(\alpha_T) = -\frac{C_1(T - T_0)}{C_2 + T - T_0} \tag{19}$$

where δ, α, η and γ are coefficients; f_R is reduced frequency ($= \alpha_T \times f$); C_1 and C_2 are WLF constants. The dynamic modulus master curves of the tested mixtures are constructed at 21 °C reference temperature. As shown in Fig. 3, laboratory-produced (AC-L, SMA-L) and aged (AC-P1-X, SMA-P2-X) mixtures have low dynamic modulus (stiffness) at high temperatures. This implies that the mixtures are more susceptible to permanent deformation than unaged and plant-produced mixtures. It is possible to verify deformability using the ratio of dissipated (loss) to the maximum stored energy per cycle ($2\pi sin\varphi$, where φ is phase angle) given in Table 3. High energy loss corresponds to high phase angle and deformability potential.

On the other hand, the dynamic modulus at low temperatures and

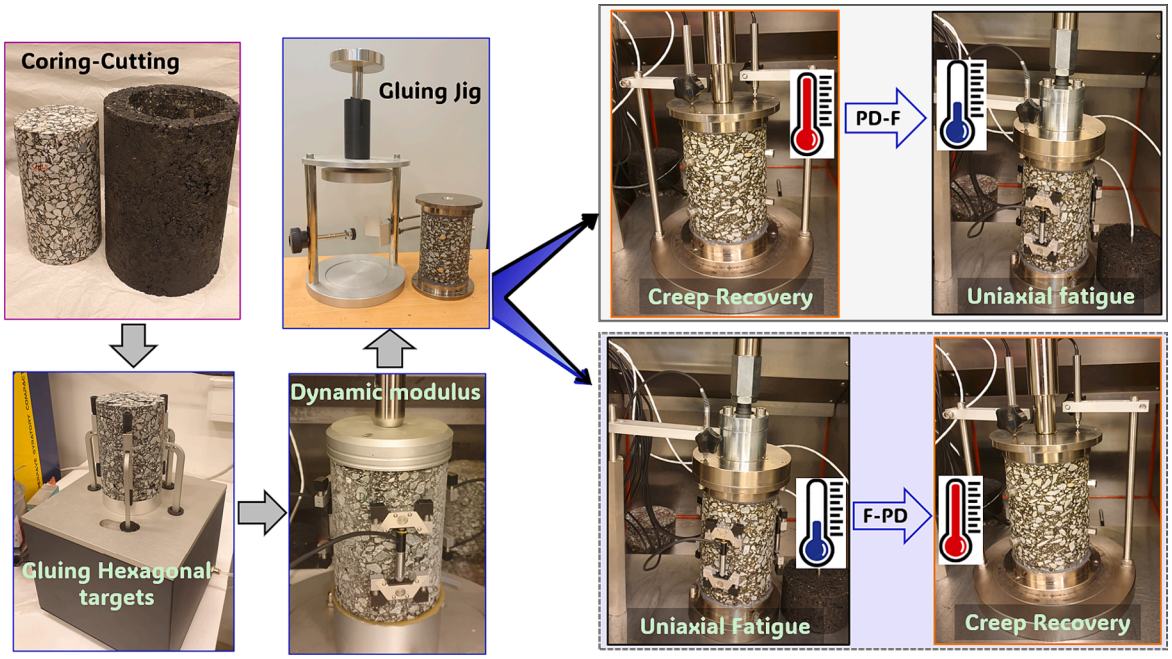

Fig. 1. Overall process testing specimen instrumentation and test sequences (dynamic modulus, creep recovery, and uniaxial fatigue tests).

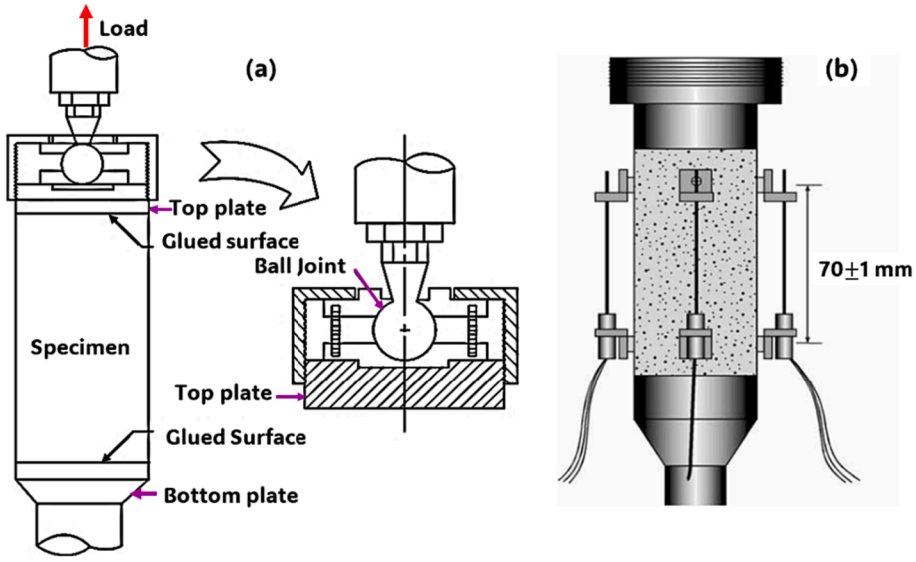

Fig. 2. Schematic of fatigue test configuration (a) locking ball joint (b) gauge point.

high frequencies corresponds to fatigue properties of mixtures. To better understand the fatigue response of the materials, the relaxation modulus curve is often used instead of dynamic modulus curve which contains the loss modulus component ($E^{''} = E^{*}sin\varphi$). Fatigue damage is the deterioration of the storage modulus due to increase in loss modulus or phase angle. For this reason, the time-domain relaxation modulus E(t) is often used to describe viscoelastic responses than the frequency-domain dynamic modulus. The relaxation modulus is obtained from the storage modulus ($E^{'}$) data using the analytical Prony method. The relaxation modulus is expressed using the Generalized Maxwell (GM) model in discrete form as follows.

$$E(t) = E_{\infty} + \sum_{i=1}^{M} E_i \left(e^{\left(-t/\rho_i\right)} \right) \tag{20}$$

where E_{∞} is long-term (equilibrium) modulus; E_i and ρ_i are relaxation modulus and relaxation time, respectively; and M is the total of number of GM elements. A total of 12 Prony series coefficients were found sufficient to fit the relaxation modulus curve using a pre-smoothened storage modulus data (Fig. 4). The pre-smoothening is done using a sigmoid-type continuous function to remove outliers in the storage modulus data [29]. The log–log ratio of the relaxation modulus – time curve is the slope, such that, the maximum slope is $m_o = \max\left\{\frac{\Delta log(E(t))}{\Delta log(t)}\right\}$. It has been established that the maximum slope is related to the viscoelastic damage rate (α), which is expressed for strain-controlled tests as $\alpha = \frac{1}{m_o} + 1$ [38]. The viscoelastic damage rate is found dependent on confining stress for triaxial test scenarios [29]. As given in Table 3, laboratory-produced mixtures (AC-L and SMA-L) have the maximum slope of relaxation modulus which corresponds to minimum damage rate (alpha). This is inline with the possibility that plant-produced mixtures could undergo oxidative aging [51] and hardening

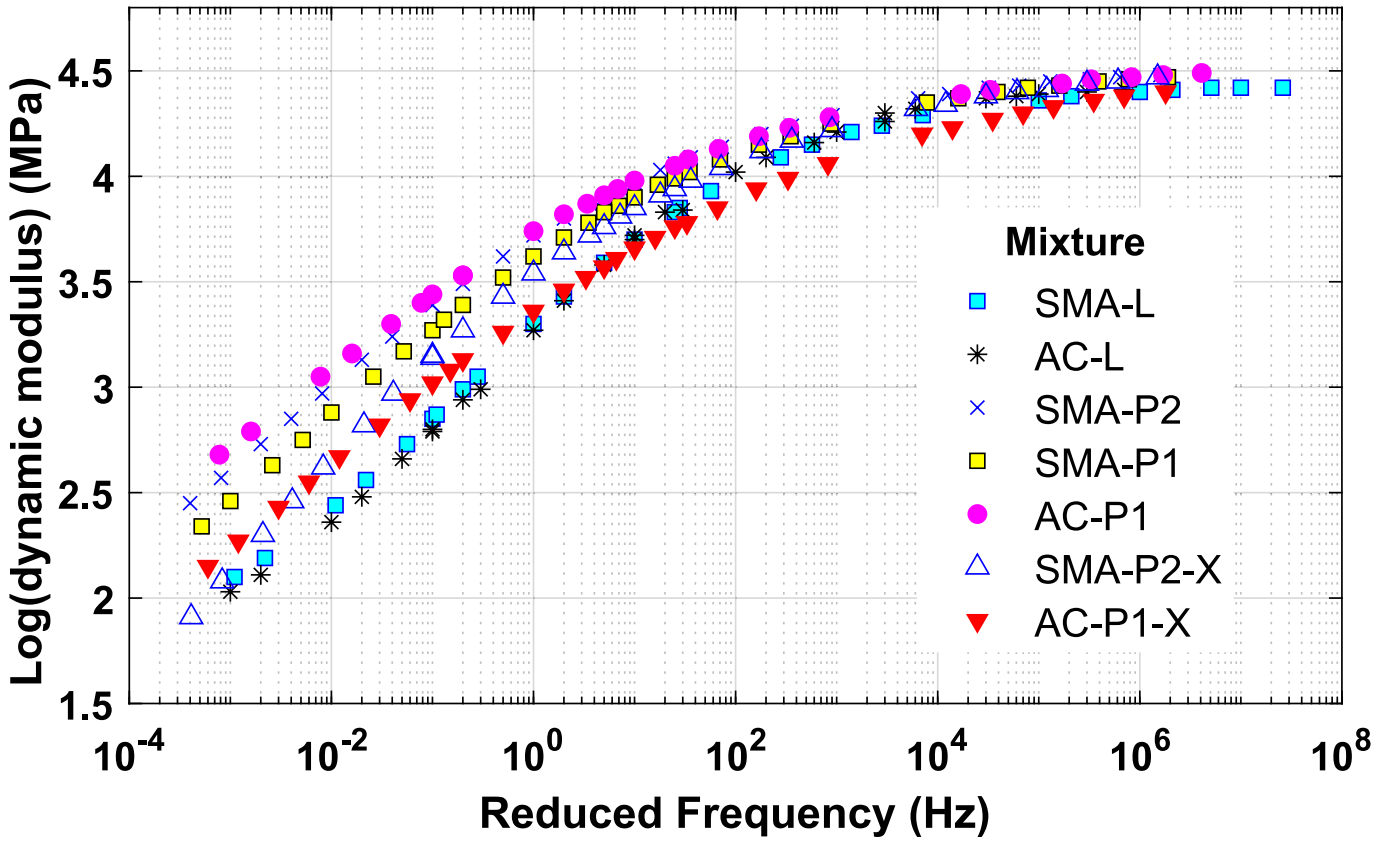

Fig. 3. Dynamic modulus master curves (reference temperature at 21 °C).

Table 3
Loss modulus ratio and relaxation modulus-related variables (long-term relaxation modulus and viscoelastic damage parameter).

	AC-L	SMA-L	AC-P1	SMA-P1	SMA-P2	AC-P1-X	SMA-P2-X
Maximum loss ratio ($2\pi\sin\varphi$)	4.09	4.08	3.61	3.831	3.76	3.84	4.25
E_∞ *(MPa)*	61.92	87.88	172.48	101.74	127.12	72.20	38.78
Maximum Slope (m_o)	0.70	0.69	0.52	0.59	0.53	0.50	0.65
Alpha (α)	2.43	2.45	2.91	2.69	2.90	3.02	2.54

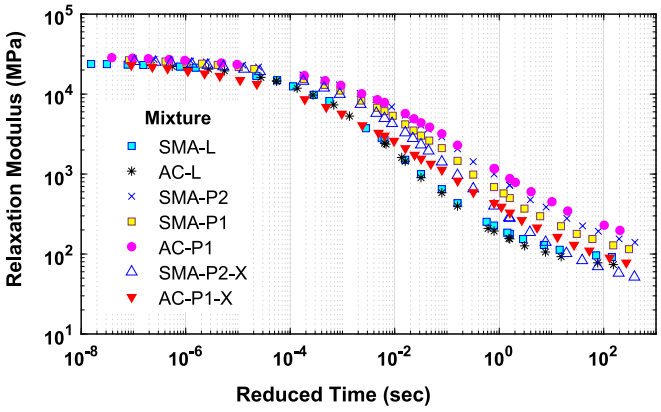

Fig. 4. Relaxation modulus master curves (reference temperature at 21 °C).

phenomena due to re-heating the loose mixture sample for gyratory compaction.

4.2. Cyclic creep-recovery test

Permanent deformation damage response of asphalt concrete is highly stress and stress-path dependent [29,52]. Stress sensitivity increases with temperature for both viscoelastic and viscoplastic responses. The creep-recovery response of asphalt concrete was explained using the strain rate in the three creep phases. In a typical asphalt mixture, the strain rate decreases in the primary stage, constant rate (steady state) in the secondary stage, and rapidly increases in the tertiary stage. The rate in the steady-state stage is the most important property to assess the performance of asphalt concrete because of the strain hardening. The tertiary stage commences with the formation of micro-cracks at the maximum saturation of strain-hardening, the flow number (FN). The FN can be identified when the second derivative of the Francken model (Eqn (4)) changes from negative to positive. After the flow number, shear failure starts at constant volume. The first part of the equation (AN^B) is the power function to fit the primary and secondary stages and the viscodamage part is fitted using ($C(e^{DN}-1)$). The coefficient *'B'* is the rate of strain in the secondary stage or the rate of hardening.

Furthermore, triaxial creep-recovery tests are selected in lieu of the uniaxial to simulate the actual field confinement. The realistic confining pressure in pavements is thought to be between 100 and 200 kPa, depending on the mixture type. The confining- and axial stress-dependent responses of asphalt concrete can be seen in Fig. 5 (a to d). The axial stress increases the rate of deformation, while confinement retards the strain rate and increases in the viscosity (λ) thus extends the flow number.

4.2.1. Four-stage permanent deformation criterion

From a mechanistic viewpoint, the classic flow number failure criterion is only an indicator for the initiation of shear deformation (viscodamage) and could not give the full history of viscoplastic damage evolution. In actual practice, pavements can be in-service after micro cracks initiated at the flow number, that is, from micro-crack initiation at **FN** to the formation of macro cracking. In this phase, the micro cracks accumulate, grow, and coalesce to cause macro cracks. Therefore, it is worth investigating the remaining life of pavement from maximum hardening saturation to the formation of macro crack, which is referred to as *shear endurance life (SEL)*. To estimate the life between FN and the macro crack formation a new formulation is proposed. Note that using the conventional strain rate method, it was not possible to identify the cycle number where macro-cracks started. The dissipated energy approach is applied to formulate a fourth creep phase in the tertiary stage and to calculate the shear endurance life, *SEL*. The cycle number at the macro-crack formation need to be revealed, which is denoted as N_{PV}. Thus, SEL is expressed as

$$SEL = N_{PV} - FN \tag{21}$$

The dissipated energy criterion DER_{PD} from Equation (17) is applied to find a peak point (cycle number) in the tertiary creep stage where the macro-crack started. As shown in Fig. 6, it is possible to reveal additional fourth creep phase in the tertiary creep stage using the dissipated energy ratio method.

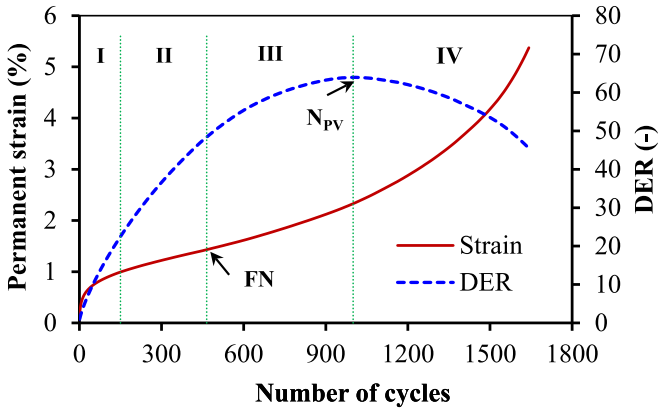

Fig. 6. Four-stage permanent deformation evolution – SMA-P2-X (T = 40 °C, σ_d = 650*kPa*).

The peak value of the DER curve (N_{PV}) is believed to be the point of macro-crack formation that corresponds to excessive energy dissipation. At this point, the shear endurance limit is reached, and the sample can carry no more external load. As the FN marks the start of micro-crack initiation, and the N_{PV} marks the formation of macro-cracks and the commencement of the fourth creep stage. The DER curve starts descending in the fourth stage due to excessive energy dissipation, which leads to loss of integrity or collapse. In the above expression (Eqn

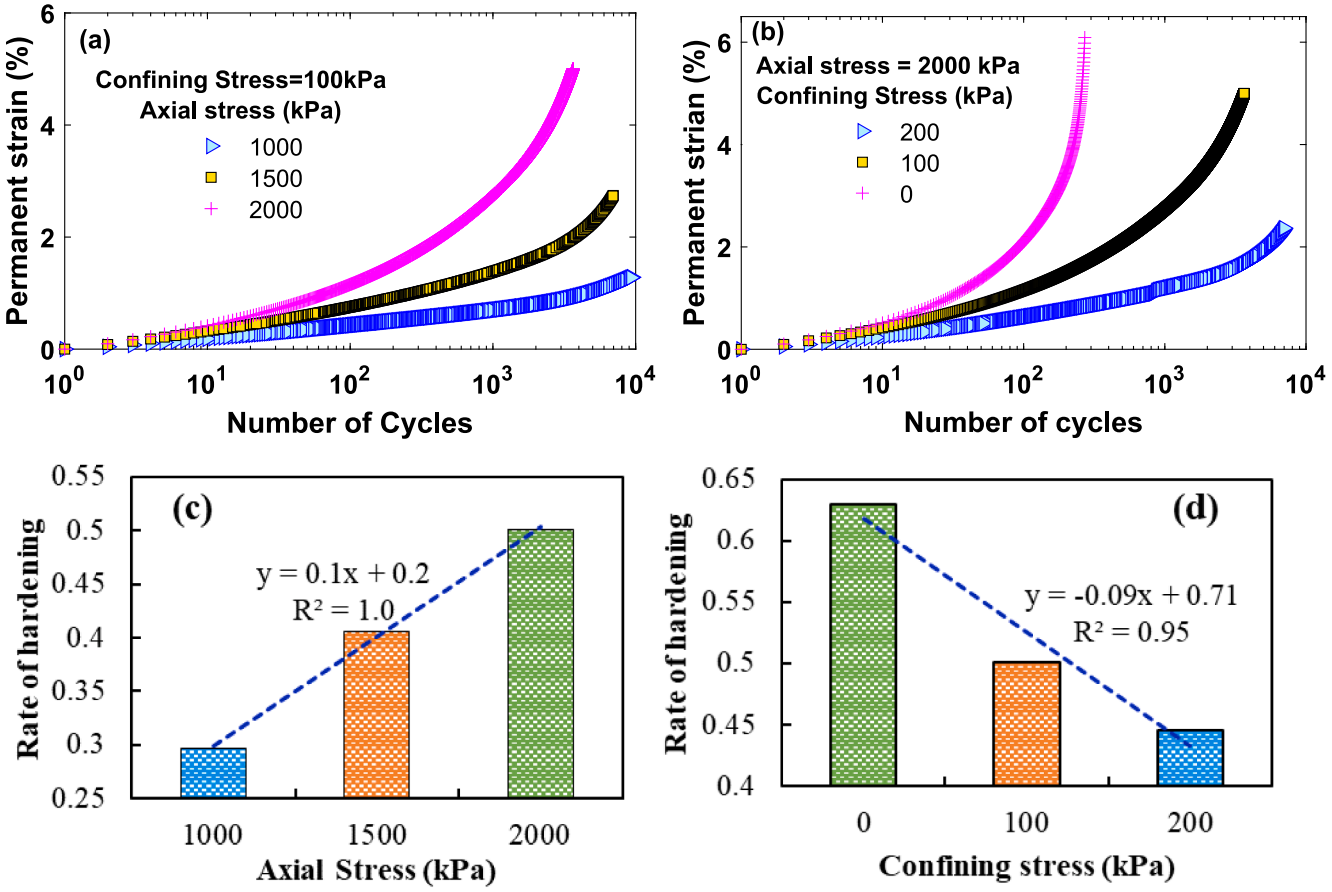

Fig. 5. Effect of stress on permanent deformation and hardening rate – (AC-P1 at 50 °C).

(21)), the corresponding permanent strains at peak point (ε_{PV}) and flow number (ε_{FN}) can be used to express the shear endurance life, $\varepsilon_{SEL} = \varepsilon_{PV} - \varepsilon_{FN}$.

An example is presented to illustrate the relation using aged specimen (SMA-P2-X). As shown in Fig. 7, a positive correlation is found between flow number and SEL and N_{PV} with good accuracy. High flow number means a long shear endurance life before macro-crack formation. The correlation between the number of cycles in Fig. 7**(a)** has shown better relationship than using the corresponding strain quantities in Fig. 7**(b)**.

Similar correlation can be seen for other six mixtures tested at different temperatures, and axial stress levels. The result presented in Fig. 8 is for the AC-P1-X mixture. The data points in the Fig. 8 represents the **SEL** and N_{PV} of tested samples at two different temperatures (30 °C and 40 °C), three axial stresses (0.65, 1.5 and 2 MPa), and new and pre-fatigued samples. Regardless of initial conditions, the correlation between the flow number and the peak value is found in agreement, but the shear endurance life (SEL) has shown slightly weak correlation. This implies that the shear deformation (viscodamage) phase is dependent on stress, temperature, and initial conditions of the specimen.

Furthermore, the deformability rates (ε_{FN}/FN, ε_{PV}/N_{PV} and ε_{SEL}/SEL) are used to assess the viscoplastic deformation rates of different mixtures. Fig. 9 shows the good correlation between the deformability rate and the flow number. The data points in the figure corresponds to flow numbers and permanent strain at maximum saturation for different AC-P1-X and SMA-P2-X duplicate samples tested at different temperatures (30 and 40 °C), and deviatoric stresses (from 0.5 to 2 MPa). Regardless of the differences with testing parameters, the deformability rate can be approximated with a power relationship.

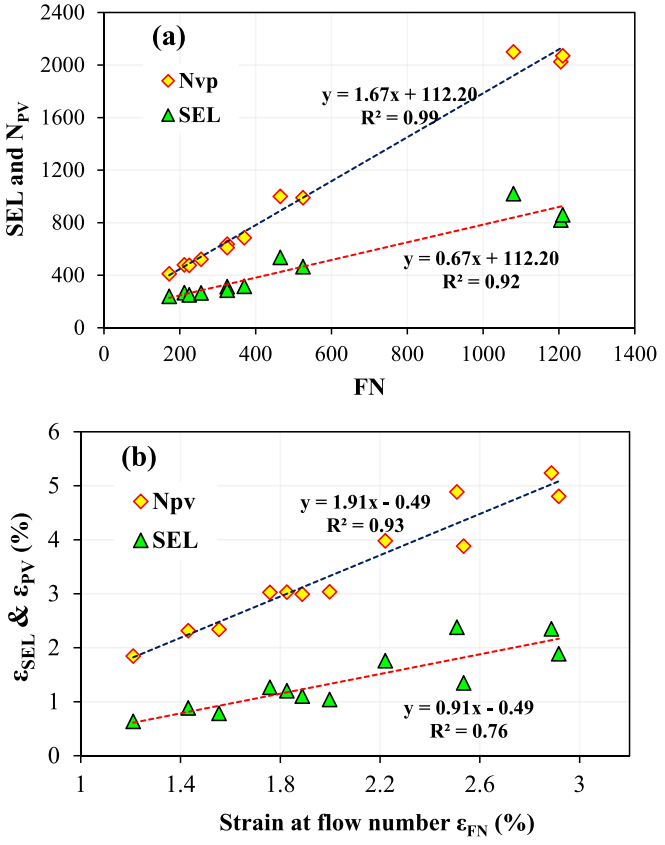

Fig. 7. Correlation between (a) cycle numbers (b) strains components – SMA-P2-X (T = 40 °C).

4.3. Uniaxial fatigue test

Uniaxial fatigue tests were conducted on different asphalt concrete mixtures on new and strain-hardened specimens according to test parameters given in Table 2. Fatigue tests are recommended between 5 and 15 °C, mostly at 10 °C [44]. Typical fatigue damage response is described using dynamic modulus deterioration curve which evolved in three stages, as shown in Fig. 10, a rapid reduction in the first phase, steady state in the second stage and a rapid reduction in the third stage.

As discussed in Section 2.3, the viscoelastic continuum damage model is the most comprehensive fatigue damage constitutive model that considers time-temperatures factor, rate of relaxation module change, factor for specimen-to-specimen variation and pseudo stiffness deterioration. Therefore, the damage characteristic curves (C – S) are constructed to characterize the pseudo stiffness deterioration (C) due to damage (S). The 50 % pseudo stiffness reduction is considered as fatigue failure point. The C-S relationship relates the temperature dependent viscoelastic damage quantity with the pseudo stiffness deterioration. As shown Fig. 11, laboratory-produced and aged specimens have shown rapid damage rate compared to that of plant produced specimens. The C – S curve can be used to classify different mixtures. However, the comparison based on the C-S curve can be misleading. For example, from rheological viewpoint, the damage rate (alpha) is smaller for laboratory and aged samples (Table 3). Several factors such as initial void (pre-flaw) can influence the damage rate. Moreover, the damage rate of the tested mixtures is consistent with the slope of relaxation modulus or the viscoelastic damage parameter (alpha).

Furthermore, the dissipated energy ratio, $DER_F = n \times \left(\frac{E_1}{E_i}\right)\left(\frac{\varphi_1}{\varphi_i}\right)$ is used to characterized the rate of damage accumulation for different fatigue tests. For the control-strain fatigue tests, the effect of target on-specimen strain is an important factor for damage rate. Fig. 12 shows examples of specimens fatigued for about 16 % to 40 % reduction of initial modulus. It is found that the DER_F curve is dependent on temperature and on-specimen control strain (με). Specimens with high damage have lower rate of DER at low temperatures. As temperature increases, DER_F decreases or fatigue resistance increases.

5. The interaction of fatigue and permanent deformation

5.1. The PD-F sequence

5.1.1. The effect of strain hardening on fatigue damage

The rational of the PD-F sequence is the assumption that permanent deformation evolves before ductility exhaustion and significant fatigue cracking in asphalt concrete, as discussed in Section 3.2.1. For instance, new pavements are more likely to undergone volumetric densification (deformation) before fatigue cracking initiates. This is due to the reason that high energy is required to initial fatigue cracking due to the fast relaxation and viscous properties of new asphalt pavements. Therefore, initial strain-hardening of the asphalt concrete can have a direct consequence on the fatigue damage rate of serviceable pavements. To investigate this scenario, asphalt concrete samples are pre-deformed in steady-state stage at 40 or 50 °C and the same sample is tested in uniaxial fatigue part of the PD-F sequential test at 10 °C and 10 Hz in tension-tension or tension-compression mode.

The objective of the PD-F test sequence is to investigate the effect of strain hardening on the fatigue damage rate of asphalt concrete mixtures. Considering the pre-deformation (strain hardening) effect during fatigue test is believed as a more realistic way of damage sequence when actual pavement is considered. In the PD part, volumetric deformation evolves (air void reduction), and the viscous nature of asphalt concrete is reduced, making the material prone to fatigue cracking. Thus, strain hardening can cause an increase in the 'nominal stiffness' of the specimen and accelerates fatigue damage. After a certain level of hardening (aging), both fatigue and permanent deformation damages can develop

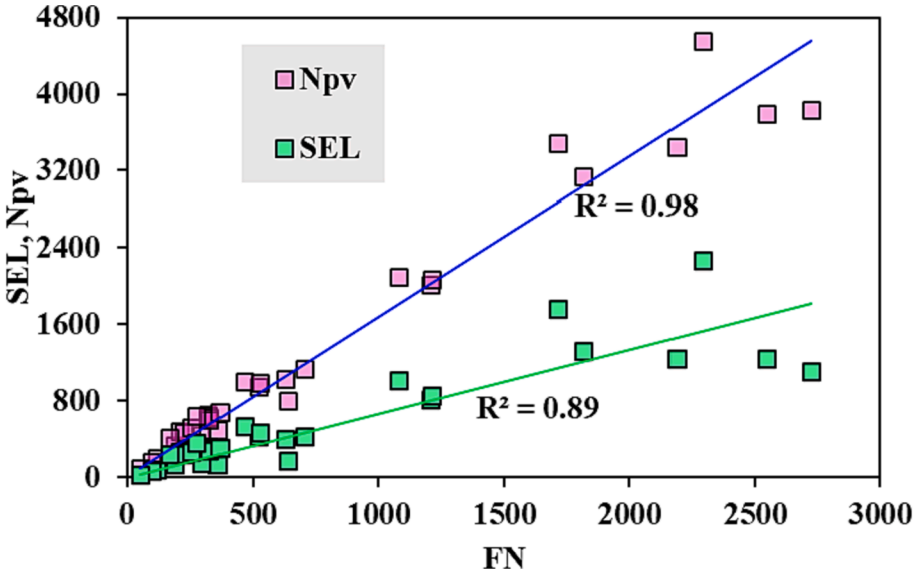

Fig. 8. Correlation between *FN*, N_{PV} and SEL – AC-P1-X.

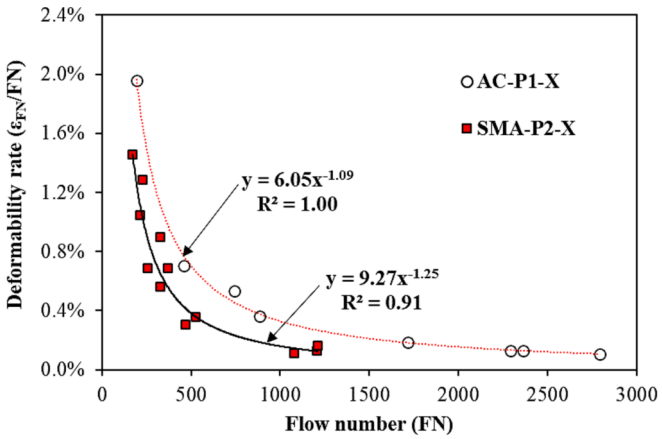

Fig. 9. Deformability rate $(\frac{\varepsilon_{FN}}{FN})$ versus flow number for different mixtures.

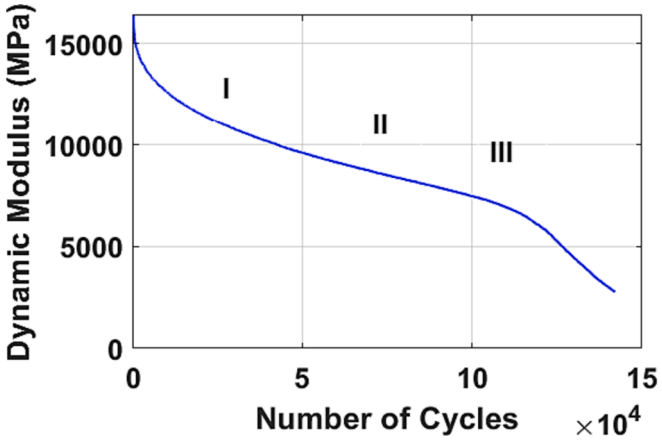

Fig. 10. Typical fatigue damage test (T = 10 °C and 300 με) – SMA-P2.

simultaneously.

The viscoelastic continuum damage (VECD) approach is applied to quantify the fatigue damage evolution. The damage characteristic curve is fitted using the expression $C = 1 - as^b$, where parameter *b* is the slope of *logC* – *logS* curve. As shown in Fig. 13, the strain hardening (PD) accelerates fatigue damage rate in the PD-F test sequence. It is evident that pre-deformed samples have shown high fatigue damage rate and energy dissipation than undeformed (new) samples. The results are consistent for the new and aged tested specimens.

Moreover, Fig. 14 (a) demonstrates that the rate of pseudo stiffness deterioration or parameter *'b'* in $C = 1 - as^b$ is used to visualize pseudo stiffness deterioration rate. This agrees with the relaxation modulus rate (maximum slope and alpha) (Fig. 4 and Table 3). Alternatively, the dissipated energy quantity can also be used to explain the PD-F interaction of fatigue and permanent deformation. As shown in Fig. 14 (b), for the same amount of pseudo stiffness reduction, the amount of cumulative dissipated energy needed is greater for new samples than the pre-deformed ones. This means the number of cycles required to cause a 50 % of pseudo stiffness reduction are smaller for pre-deformed (strain hardened) samples than the new (undeformed) specimens. In other words, the amount of energy expended on new samples is much higher than the pre-deformed samples to cause failure. Thus, both the dissipated energy and continuum damage approaches yield similar conclusions (Fig. 14 a and b).

The cumulative damage variable (S) at 50 % pseudo stiffness reduction and the dissipated energy quantity (DE_F) give some comparable regression and good correlation, as shown in Fig. 15. The correlation could be perfect linear. However, the damage (S) is the aggregate of all internal state variables including any viscoplastic deformation and viscous while the DE_F is the energy expended due to an assumed pure sinusoidal load only.

5.2. The F-PD sequence

5.2.1. The effect of pre-fatigue cracking on permanent deformation

As discussed in Section 3.2.1, the objective of the F-PD sequence test is to investigate the effect of pre-existing fatigue crack on the permanent deformation responses of different asphalt concrete mixtures. First, the fatigue part of the F-PD sequence is conducted at 10 Hz frequency and 10 °C temperature to induce a certain extent of fatigue cracking (maximum of 40 % dynamic modulus reduction). Then, the same pre-fatigued specimen is test in a creep-recovery permanent deformation test at higher temperature (30, 40 and 50 °C) until failure. The fatigue part of the F-PD test sequence is intended only to cause initial cracks not to fail the sample in a controlled-strain test prior to creep-recovery test. It is possible that viscoplastic deformation can develop during the

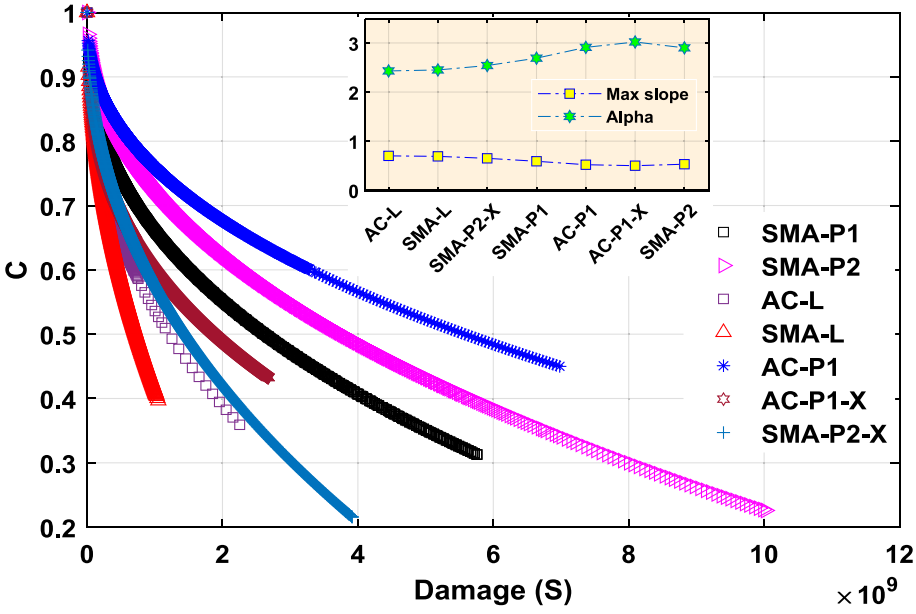

Fig. 11. Fatigue damage characteristics (T = 10 °C and Target strain = 300 με).

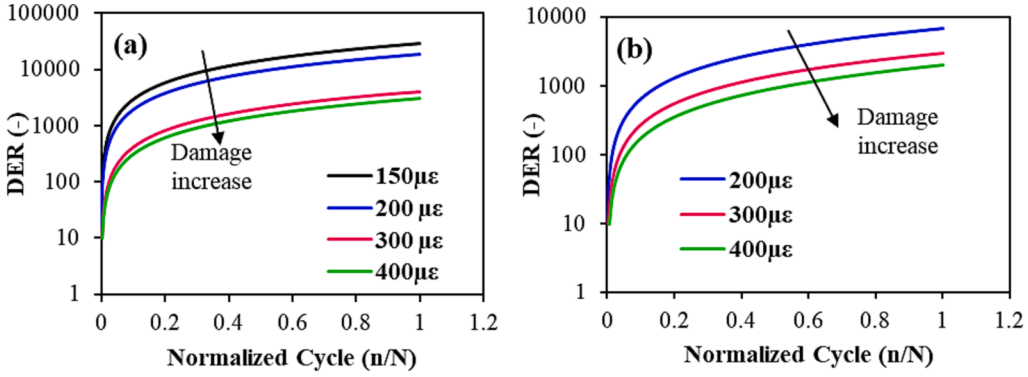

Fig. 12. DER_F for T-C fatigue test at different control-strain (SMA-P2-X) (a) 10 °C (b) 15 °C.

fatigue part of the tests. However, it is highly dependent on the fatigue test temperature and target on-specimen strain amplitude. It is found that a tension–compression fatigue test at 10 °C caused no more than 0.08 % creep strain. Thus, the corresponding dissipated energy due to the creep strain is insignificant compared to the cyclic fatigue part [43].

The effect of pre-existing cracking on permanent deformation in the F-PD sequence is analyzed using the strain rate in the steady-state stage, flow number and the expanded energy. The dissipated energy and hardening rate are strongly dependent on the deviatoric stress. High deviatoric stress result in high dissipation, rapid creep rate, and small flow number. First, the deformation (hardening rate) is studied with respect to the energy quantities in the F-PD sequence. It can be seen in Fig. 16 **(a)** that the strain hardening (parameter *'B'* in Francken model) is positively proportional with the dissipated energy due to creep-recovery deformation (where $\boldsymbol{DE_{PD}}$ is the cumulative energy up to flow number). However, the rate of strain hardening has a negative correlation with the dissipated energy due to fatigue ($\boldsymbol{DE_F}$) in the F-PD sequence (Fig. 16 b). In addition, the effect of pre-fatigue on permanent deformation is analyzed by correlating the flow number and respected expended energies in fatigue and permanent deformation damages ($\boldsymbol{DE_F}$ and $\boldsymbol{DE_{PD}}$).

It is also found that neither DE_F nor DE_{PD} energy quantities are consistent with the flow number, as shown in Fig. 17. The expended energies are dependent on mixture type and temperature. In Fig. 17**a**, the DE_{PD} at 30°C shows an increasing trend for AC-P1-X mixture. On the other hand, it has a decreasing relation for the SMA-P2-X at 40 °C with respect to flow number (Fig. 17**b**). The DE_{PD} is high for a small flow number, that is, deformation rate is high due to rapid permanent deformation at higher temperature (Fig. 17**b**). It should be emphasized here that comparison based on energy dissipation quantity alone is difficult and could give misleading conclusions. It also varies from specimen to specimen, initial voids, and pre-fatigue damage. Several phenomena can be the reasons for the inconsistency of the effect of fatigue on the subsequent permanent deformation damage. Firstly, the PD part of F-PD test is performed at higher temperatures (30, 40 and 50 °C) and some of the initial fatigue cracks (at 10 °C) can heal during the rest period and temperature conditioning period for the creep-recovery tests. However, energy dissipation is irreversible regardless of the sample's apparent (damage) state or the healing potential. Secondly, the tension–compression or tension–tension cyclic fatigue test using cylindrical specimens requires large loading cycle to cause significant cracks (the 50 % stiffness reduction is only an approximate failure criteria). Therefore, 20 to 40 % stiffness reduction in fatigue tests has little impact on the subsequent permanent deformation damage. The third reason could be related to potential hardening or post compaction during the tension–compression fatigue test phase. This compaction can improve deformation resistance. Thus, based on this study, the effect of small pre-crack on the permanent deformation (F-PD sequence) is found marginal.

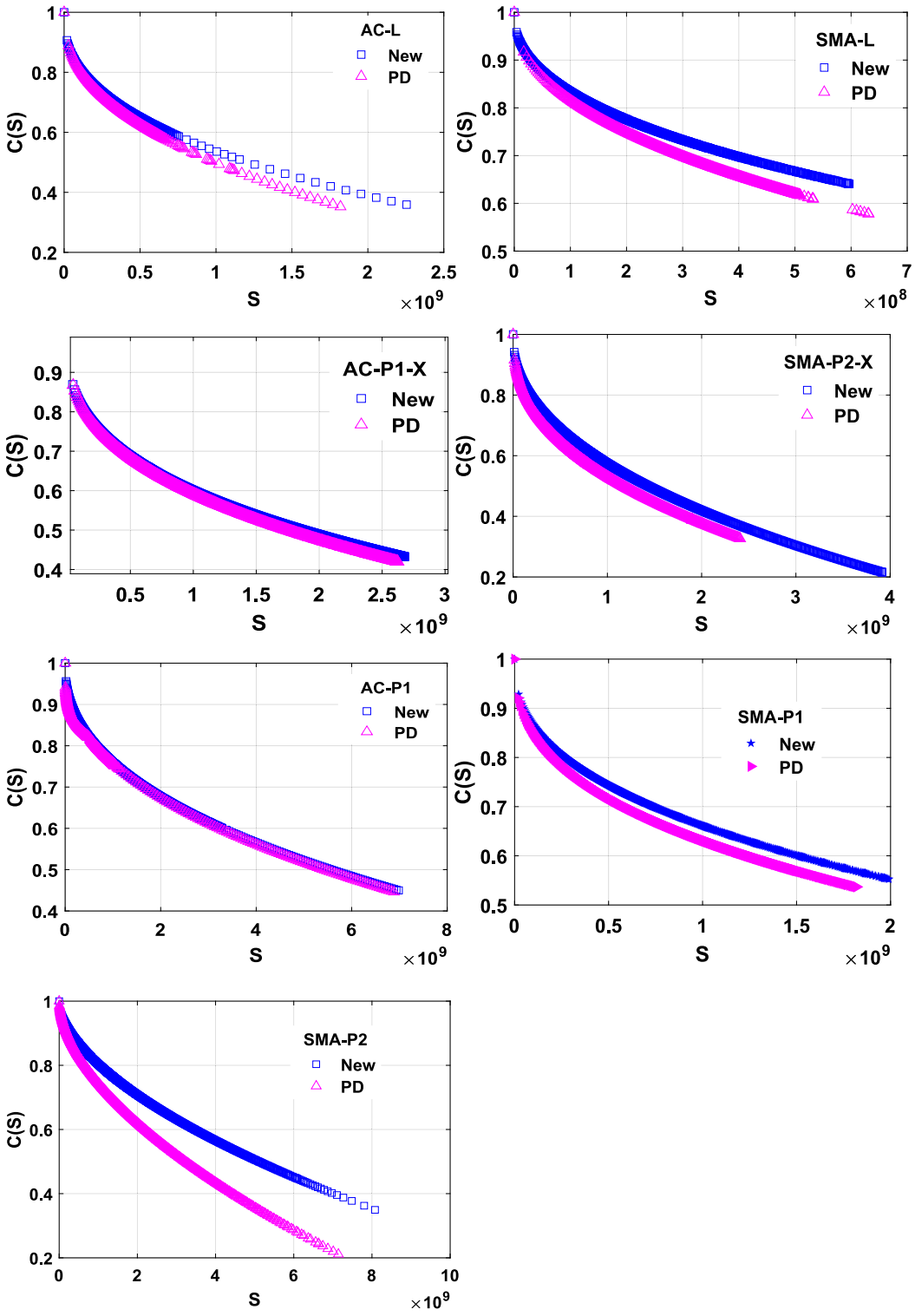

Fig. 13. PD-F sequence - fatigue damage characteristics (T = 10 °C and target strain 300 με) of new and per-deformed (PD) asphalt mixtures.

5.3. Total dissipated energy

Based on the sequential procedure, the total dissipated energy (DE_T) can be the discrete sum of expended energies on each test specimen. A simple linear summation can be assumed ($DE_T = DE_{PD} + DE_F$). Different behaviors of asphalt concrete such as hardening relaxation, healing, aging etc., can significantly affect the interaction between fatigue and permanent deformation in both the PD-F and F-PD sequences. The effect of temperature and role of material type is also crucial for energy dissipation. The magnitude of DE_F is found much smaller than the DE_{PD} for both the F-PD and PD-F sequences (Fig. 17). This can be due to the reason that the fatigue test is conducted in strain-controlled mode and the expended energy per cycle DE_F is much smaller than DE_{PD}. On the other hand, the DE_{PD} is a stress-controlled test at high temperature. Thus, DE_T decreases as the flow number increases for the same amount of fatigue damage (DE_F). Fig. 18 shows the total expended energy for the F-PD sequence. The mixtures AC-P1-X and SMA-P2-X are used to explain the F-PD test sequence. The fatigue part is tested at 10 °C, and the PD

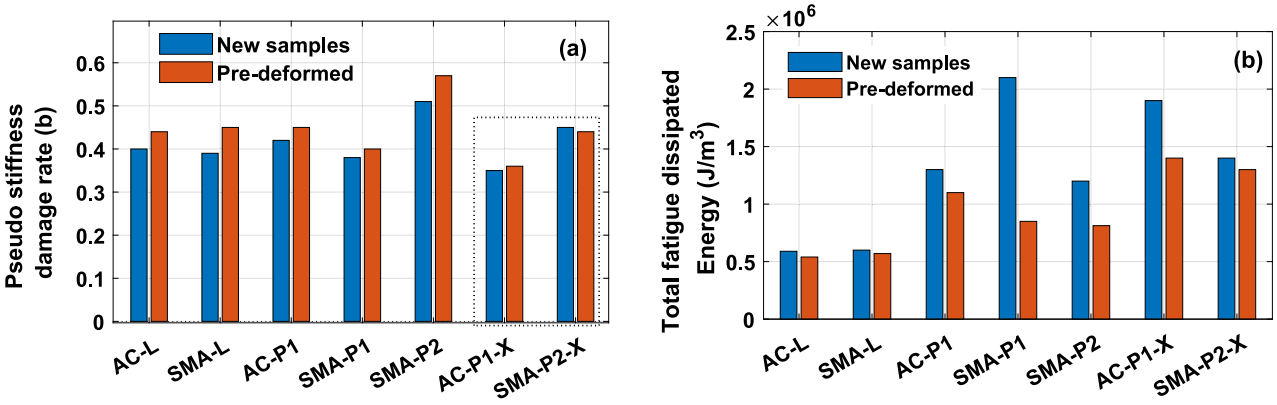

Fig. 14. Effect of pre-deformation on fatigue damage responses (a) parameter *b* (b) total fatigue dissipated energy until failure (50% pseudo stiffness).

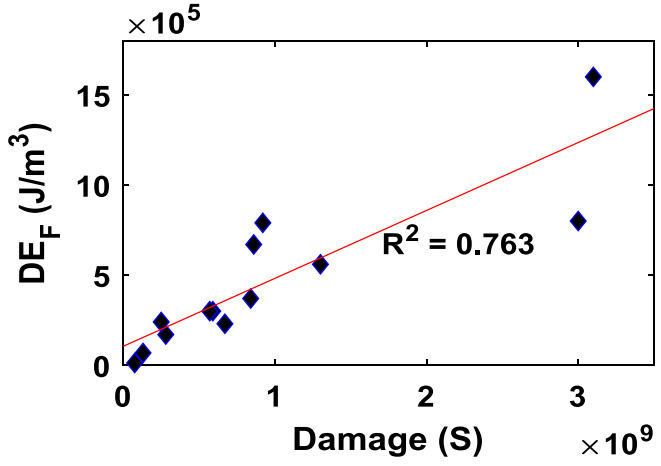

Fig. 15. Damage variable S and dissipated energy DE_F on new samples – AC-P1-X. *Note: the data points are for different samples tested at different controlled-strain levels.*

part is at 30 °C and 40 °C for fatigue and permanent deformation. Based on a simple additive of energies, inconsistency with respect to the flow number is observed (Fig. 18). The dissipation rate is defined as the ratio of total dissipated energy to the corresponding flow number $\left(\frac{DE_T}{FN}\right)$ and indicate a descending pattern with flow number for both mixtures, as shown in Fig. 18 (**a** and **b**). It should be underlined that the total dissipation energy is dependent on sequence and the damage interaction will affect the total dissipated energy in a nonlinear manner both in the F-PD and PD-F sequences. Hence, the total dissipated energies in the two sequences (DE_{F-PD} and DE_{PD-F}) will be different.

5.4. Discussion

The mechanistic prediction of damage in asphalt pavement has been the focus of study in last recent decades. Asphalt concrete is exposed to cyclic load from traffic and undergo a creep-recovery process in its service life, and two main damage evolve in the form of stiffness deterioration (fatigue cracking) and viscoplastic strain (permanent deformation). From the literature study, it is evident that the interaction between these two dominant damage modes was not presented in detailed. However, field observations have shown the mutual progression of the two damage on the pavement surface along the longitudinal wheel path.

In this study, the experimental investigation of seven different asphalt mixtures is conducted by testing each specimen for fatigue and then for permanent deformation at low and high temperatures respectively and vice versa. The sequential test procedure is proposed to introduce the effect of pre-cracking on the permanent deformation response (in the F-PD sequence) and strain-hardening on the fatigue cracking (in the PD-F sequence). Here, temperature is considered as a factor in the sequential damage and for the testing. Most standard laboratory tests utilize gyratory compacted samples for fatigue and permanent deformation due the difficulty of getting field cored samples longer than 40- or 50-mm for fatigue and permanent deformation tests. The sequential test approach can be used to resolve and investigate the influence of pre-fatigue on deformation and vice versa using longer sample sizes. Thus, the consideration of strain hardening in fatigue test and the pre-cracking in permanent deformation is a reasonable way to characterize interaction between the two damages and try to simulate the field condition.

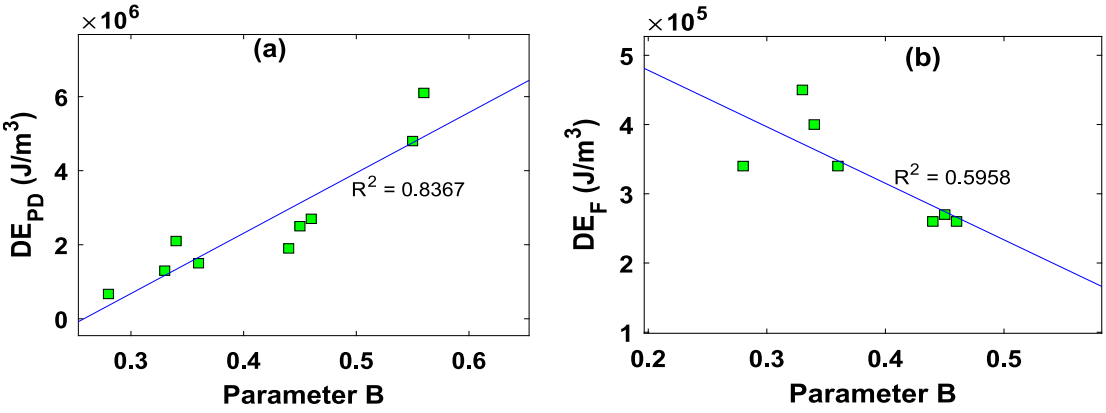

Fig. 16. Effect of pre-fatigue damage on permanent deformation rate – the F-PD sequence *(a)* DE_{PD} *of pre-fatigued samples (b) initial* DE_F *of samples used for PD test.*

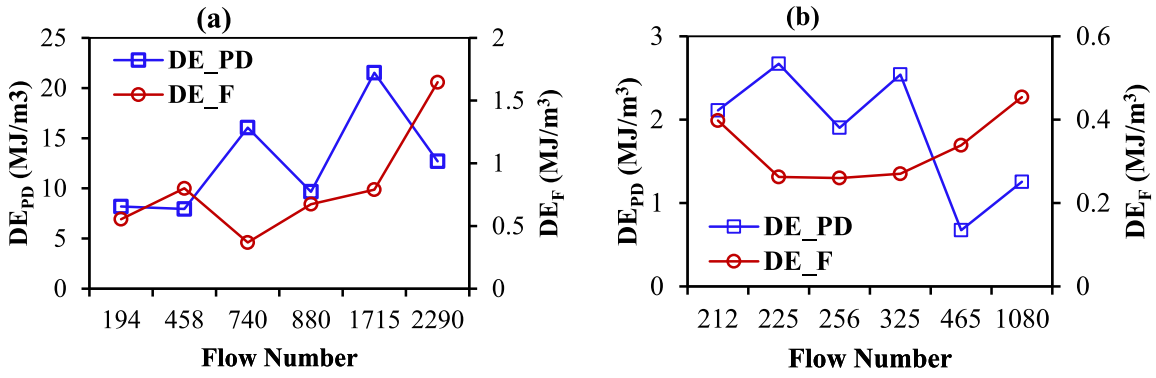

Fig. 17. Dissipated energies of pre-fatigued samples in F-PD sequence: *(a) AC-P1-X fatigue at 10 °C and PD at 30 °C and 2 MPa (b) SMA-P2-X fatigue at 10 °C and PD at 40 °C, 0.65 MPa.*

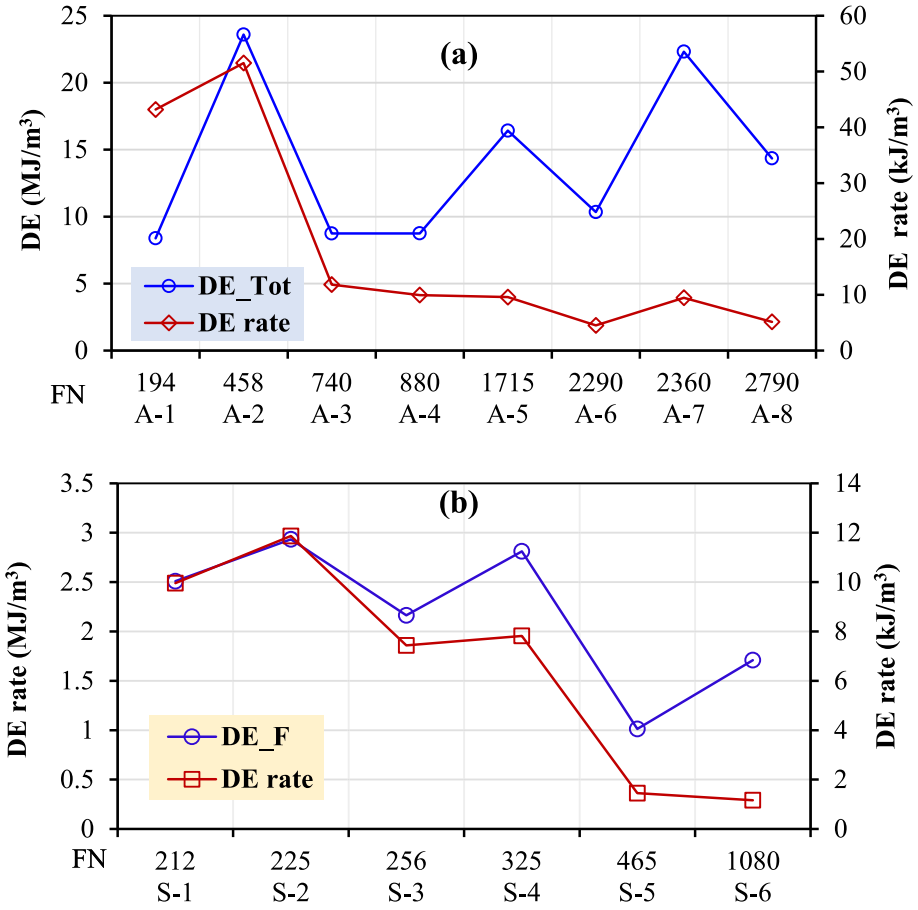

Fig. 18. Correlation of total dissipated energy and flow numbers in F-PD sequence (a) AC-P1-X, PD at 30 °C (b) SMA-P2-X, PD at 40 °C.

First, the linear viscoelastic responses of mixes are analyzed using dynamic modulus test and the time–temperature superposition principle. The respective damages are quantified using the energy and continuum approaches. In the energy approach, the total dissipated energy is computed by assuming a simple linear addition of expended energies on each specimen tested in F-PD and PD-F sequences. The discreteness of energy per cycle is an advantage for simplicity but can be inefficient to consider the microstructural changes in a continuous time history. The interaction between deformation and fatigue damages is believed to be a complex phenomenon due to the thermo-piezo-rheological, healing, hardening-relaxation behaviors of asphaltic materials. The continuum method is the most comprehensive method for the time-dependent (history) of damage evolution and has the advantage of damage coupling in continua.

From experimental observation and analyses, the PD-F sequence is more plausible and suitable for experimentation, and the continuum method is applied conveniently to model the fatigue part of the sequence (section 5.1.1). In most pavements, permanent deformation expected before fatigue cracking initiation. The PD part of test in the PD-F sequence should be performed with attention so that the specimen will not fail beyond steady-state stage or flow number. Some asphalt mixes may not have all the three distinct creep phases. Therefore, the PD part of PD-F sequence needs careful consideration so that only strain hardening is induced not micro-cracks in the specimen. On the other hand, the F-PD sequence is observed to be challenging to quantify the effect of fatigue cracking on the permanent deformation due to

relaxation and healing effects at high temperature during conditioning.

Furthermore, the sequential test approach offers saving in both material and sample preparation time. A single specimen is utilized for three tests i.e., dynamic modulus, fatigue, and creep-recovery (depending on either the F-PD or PD-F sequence). A framework can be developed and standardized to investigate the sequential test procedure for various levels of pre-deformation or pre-crack as a function of material properties, temperature, stress and strain levels, etc. In general, the study explored the interaction of fatigue and permanent deformation damages and verified the proposed test procedure and models using extensive test data from seven asphalt mixtures produced in laboratory and mixes collected from asphalt production plants.

6. Conclusion

The focus of this study is the experimental investigation of permanent deformation and fatigue damage of asphalt concrete mixes using repeated creep–recovery and uniaxial fatigue tests, respectively. The interaction between the two damage was explored using the energy and continuum approaches on seven asphalt mixes.

- A new permanent deformation failure criterion is proposed using the dissipated energy ratio (DER) and validated using different new and aged asphalt concrete samples. A new post flow number creep phase is found in the shear deformation stage that marks the formation of macro-cracks at the end of shear endurance limit.
- A sequential test procedure (STP) is proposed to investigate the interaction between fatigue (F) and permanent deformation (PD) damage in two orders – *the F-PD and PD-F sequences*. The sequential damage assumption is found simple and effective approach to characterize damage interaction using the existing conventional test protocols.
- The PD-F sequence has shown that permanent deformation (*strain hardening*) is the cause high fatigue damage rate, which agrees with the literature and field observations. The finding ascertains that the fatigue test using new samples can overestimate fatigue life of asphalt mixtures.
- In the F-PD sequence, the effect of pre-fatigue cracking up to 40 % initial stiffness at low or intermediate temperatures is found marginal on permanent deformation at 30 °C and 40 °C. Healing and relaxation are the likely reasons for this phenomenon.
- Aged and laboratory mixed samples are found prone to high fatigue damage, and the effect of strain hardening on fatigue is highly pronounced on stone mastic asphalt (SMA).
- The energy method is simple and straightforward, but the discreteness of energy quantity can be the limitation for accurate characterization of damage in continua. A nonlinear interactive damage model should be considered for accurate time-history characterization of fatigue-permanent deformation interaction.

CRediT authorship contribution statement

Mequanent Mulugeta Alamnie: Conceptualization, Methodology, Data curation, Writing – original draft, Visualization. **Ephrem Taddesse:** Conceptualization, Supervision, Writing – review & editing. **Inge Hoff:** Conceptualization, Supervision, Writing – review & editing.

Declaration of Competing Interest

The authors declare the following financial interests/personal relationships which may be considered as potential competing interests: Mequanent Mulugeta Alamnie reports financial support was provided by University of Agder Department of Engineering sciences.

Data availability

Data will be made available on request.

References

[1] M. Zaumanis, L.D. Poulikakos, M.N. Partl, Performance-based design of asphalt mixtures and review of key parameters, Materials & Design 141 (2018) 185–201.
[2] N. Roy, A. Veeraragavan, J.M. Krishnan, Influence of confinement pressure and air voids on the repeated creep and recovery of asphalt concrete mixtures, International Journal of Pavement Engineering 17 (2) (2016) 133–147.
[3] D. Perraton, H. Di Benedetto, C. Sauzéat, C. De La Roche, W. Bankowski, M. Partl, J. Grenfell, Rutting of bituminous mixtures: wheel tracking tests campaign analysis, Materials and Structures 44 (5) (2011) 969–986.
[4] J. Lundberg, S. Janhäll, M. Gustafsson, S. Erlingsson, Calibration of the swedish studded tyre abrasion wear prediction model with implication for the NORTRIP road dust emission model, International Journal of Pavement Engineering (2019) 1–15.
[5] H. Di Benedetto, T. Gabet, J. Grenfell, D. Perraton, C. Sauzéat, D. Bodin, Mechanical testing of bituminous mixtures, Springer, Netherlands, 2013, pp. 143–256.
[6] M.M. Karimi, N. Tabatabaee, B. Jahangiri, M.K. Darabi, Constitutive modeling of hardening-relaxation response of asphalt concrete in cyclic compressive loading, Construction and Building Materials 137 (2017) 169–184.
[7] V. Subramanian, M.N. Guddati, Y. Richard Kim, A viscoplastic model for rate-dependent hardening for asphalt concrete in compression, Mechanics of Materials 59 (2013) 142–159.
[8] M.K. Darabi, R.K. Abu Al-Rub, E.A. Masad, C.-W. Huang, D.N. Little, A modified viscoplastic model to predict the permanent deformation of asphaltic materials under cyclic-compression loading at high temperatures, International Journal of Plasticity 35 (2012) 100–134.
[9] F. Zhou, T. Scullion, Discussion: Three stages of permanent deformation curve and rutting model, International Journal of Pavement Engineering 3 (4) (2002) 251–260.
[10] H. Fang, Q. Liu, L. Mo, B. Javilla, B. Shu, S. Wu, Characterization of three-stage rutting development of asphalt mixtures, Construction and Building Materials 154 (2017) 340–348.
[11] M. Ameri, A.H. Sheikhmotevali, A. Fasihpour, Evaluation and comparison of flow number calculation methods, Road Materials and Pavement Design 15 (1) (2014) 182–206.
[12] Y. Zhang, R. Luo, R.L. Lytton, Characterizing permanent deformation and fracture of asphalt mixtures by using compressive dynamic modulus tests, Journal of Materials in Civil Engineering 24 (7) (2012) 898–906.
[13] M. Gajewski, W. Bańkowski, A.C. Pronk, Evaluation of fatigue life of high modulus asphalt concrete with use of three different definitions, International Journal of Pavement Engineering 21 (14) (2020) 1717–1728.
[14] S. Son, I.M. Said, I.L. Al-Qadi, Fracture properties of asphalt concrete under various displacement conditions and temperatures, Construction and Building Materials 222 (2019) 332–341.
[15] M. Ling, X. Luo, Y. Chen, F. Gu, R.L. Lytton, Mechanistic-empirical models for top-down cracking initiation of asphalt pavements, International Journal of Pavement Engineering (2018) 1–10.
[16] E.F. de Freitas, P. Pereira, L. Picado-Santos, A.T. Papagiannakis, Effect of construction quality, temperature, and rutting on initiation of Top-Down cracking, Transportation Research Record 1929 (1) (2005) 174–182.
[17] L. Ann Myers, R. Roque, B. Birgisson, Propagation mechanisms for Surface-Initiated longitudinal wheelpath cracks, Transportation Research Record 1778 (1) (2001) 113–122.
[18] X. Luo, F. Gu, M. Ling, R.L. Lytton, Review of mechanistic-empirical modeling of top-down cracking in asphalt pavements, Construction and Building Materials 191 (2018) 1053–1070.
[19] S. Mun, M.N. Guddati, Y.R. Kim, Fatigue cracking mechanisms in asphalt pavements with viscoelastic continuum damage Finite-Element program, Transportation Research Record: Journal of the Transportation Research Board 1896 (1) (2004) 96–106.
[20] I. Onifade, B. Birgisson, R. Balieu, Energy-based damage and fracture framework for viscoelastic asphalt concrete, Engineering Fracture Mechanics 145 (2015) 67–85.
[21] X. Luo, R. Luo, R.L. Lytton, Characterization of fatigue damage in asphalt mixtures using pseudostrain energy, Journal of Materials in Civil Engineering 25 (2) (2013) 208–218.
[22] T. Svasdisant, M. Schorsch, G.Y. Baladi, S. Pinyosunun, Mechanistic analysis of Top-Down cracks in asphalt pavements, Transportation Research Record: Journal of the Transportation Research Board 1809 (1) (2002) 126–136.
[23] X. Luo, R. Luo, R.L. Lytton, Energy-based mechanistic approach for damage characterization of pre-flawed visco-elasto-plastic materials, Mechanics of Materials 70 (2014) 18–32.
[24] Y. Zhang, X. Luo, R. Luo, R.L. Lytton, Crack initiation in asphalt mixtures under external compressive loads, Construction and Building Materials 72 (2014) 94–103.
[25] M.K. Darabi, R.K. Abu Al-Rub, E.A. Masad, C.-W. Huang, D.N. Little, A thermo-viscoelastic–viscoplastic–viscodamage constitutive model for asphaltic materials, International Journal of Solids and Structures 48 (1) (2011) 191–207.

[26] M. Alamnie, E. Taddesse, I. Hoff, Permanent deformation and fatigue damage interaction in asphalt concrete using energy approach, Eleventh International Conference on the Bearing Capacity of Roads, Railways and Airfields, Volume 3 (2022) 118–127.
[27] E. Levenberg, J. Uzan, Triaxial Small-Strain Viscoelastic-Viscoplastic modeling of asphalt aggregate mixes, Mechanics of Time-Dependent Materials 8 (4) (2004) 365–384.
[28] A. Graziani, F. Cardone, A. Virgili, F. Canestrari, Linear viscoelastic characterisation of bituminous mixtures using random stress excitations, Road Materials and Pavement Design 20 (sup1) (2019) S390–S408.
[29] M.M. Alamnie, E. Taddesse, I. Hoff, Thermo-piezo-rheological characterization of asphalt concrete, Construction and Building Materials 329 (2022), 127106.
[30] R. Luo, H. Liu, Y. Zhang, Characterization of linear viscoelastic, nonlinear viscoelastic and damage stages of asphalt mixtures, Construction and Building Materials 125 (2016) 72–80.
[31] W. Cao, Y.R. Kim, A viscoplastic model for the confined permanent deformation of asphalt concrete in compression, Mechanics of Materials 92 (2016) 235–247.
[32] J. Zhang, Z. Fan, K. Fang, J. Pei, L. Xu, Development and validation of nonlinear viscoelastic damage (NLVED) model for three-stage permanent deformation of asphalt concrete, Construction and Building Materials 102 (2016) 384–392.
[33] M.M. Alamnie, E. Taddesse, I. Hoff, Advances in permanent deformation modeling of asphalt concrete—A review, Materials 15 (10) (2022) 3480.
[34] R.A. Schapery, Nonlinear viscoelastic and viscoplastic constitutive equations with growing damage, International Journal of Fracture 97 (1/4) (1999) 33–66.
[35] N.H. Gibson, C.W. Schwartz, R.A. Schapery, M.W. Witczak, Viscoelastic, viscoplastic, and damage modeling of asphalt concrete in unconfined compression, Transportation Research Record: Journal of the Transportation Research Board 1860 (1) (2003) 3–15.
[36] R.A. Schapery, Correspondence principles and a generalizedJ integral for large deformation and fracture analysis of viscoelastic media, International Journal of Fracture 25 (3) (1984) 195–223.
[37] R. Schapery, A theory of mechanical behavior of elastic media with growing damage and other changes in structure, Journal of the Mechanics and Physics of Solids 38 (2) (1990) 215–253.
[38] H.-J. Lee, J.S. Daniel, Y.R. Kim, Continuum damage Mechanics-Based fatigue model of asphalt concrete, Journal of Materials in Civil Engineering 12 (2) (2000) 105–112.
[39] B.S. Underwood, C. Baek, Y.R. Kim, Simplified viscoelastic continuum damage model as platform for asphalt concrete fatigue analysis, Transportation Research Record: Journal of the Transportation Research Board 2296 (1) (2012) 36–45.
[40] Y.R. Kim, M.N. Guddati, B.S. Underwood, T.Y. Yun, V. Subramanian, S. Savadatti, Development of a multiaxial viscoelastoplastic continuum damage model for asphalt mixtures, in: C. North Carolina State University. Dept. of Civil, E. Environmental (Eds.) Federal Highway Administration, 2009.
[41] B.S. Underwood, Y.R. Kim, M.N. Guddati, Improved calculation method of damage parameter in viscoelastic continuum damage model, international Journal of Pavement Engineering 11 (6) (2010) 459–476.
[42] J.S. Daniel, Y.R. Kim, Development of a simplified fatigue test and analysis procedure using a viscoelastic, continuum damage model (with discussion), Journal of the Association of Asphalt Paving Technologists 71 (2002).
[43] E. Masad, V.T.F. Castelo Branco, D.N. Little, R. Lytton, A unified method for the analysis of controlled-strain and controlled-stress fatigue testing, International Journal of Pavement Engineering 9 (4) (2008) 233–246.
[44] S. Shen, G.D. Airey, S.H. Carpenter, H. Huang, A dissipated energy approach to fatigue evaluation, Road Materials and Pavement Design 7 (1) (2006) 47–69.
[45] K.A. Ghuzlan, S.H. Carpenter, Energy-Derived, Damage-Based failure criterion for fatigue testing, Transportation Research Record: Journal of the Transportation Research Board 1723 (1) (2000) 141–149.
[46] M. Shadman, H. Ziari, Laboratory evaluation of fatigue life characteristics of polymer modified porous asphalt: A dissipated energy approach, Construction and Building Materials 138 (2017) 434–440.
[47] J. Lemaitre, A. Plumtree, Application of damage concepts to predict Creep-Fatigue failures, Journal of Engineering Materials and Technology 101 (3) (1979) 284–292.
[48] R.P. Skelton, D. Gandy, Creep – fatigue damage accumulation and interaction diagram based on metallographic interpretation of mechanisms, Materials at High Temperatures 25 (1) (2008) 27–54.
[49] H. Di Benedetto, C. De La Roche, H. Baaj, A. Pronk, R. Lundström, Fatigue of bituminous mixtures, Materials and Structures 37 (3) (2004) 202–216.
[50] M.L. Williams, R.F. Landel, J.D. Ferry, The temperature dependence of relaxation mechanisms in amorphous polymers and other glass-forming liquids, Journal of the American Chemical society 77 (14) (1955) 3701–3707.
[51] E. Rahmani, M.K. Darabi, D.N. Little, E.A. Masad, Constitutive modeling of coupled aging-viscoelastic response of asphalt concrete, Construction and Building Materials 131 (2017) 1–15.
[52] J. Blanc, T. Gabet, P. Hornych, J.-M. Piau, H. Di Benedetto, Cyclic triaxial tests on bituminous mixtures, Road Materials and Pavement Design 16 (1) (2014) 46–69.